Preclinical validation and mechanistic understanding of drug repurposing candidates for polycystic kidney disease

Kanhai, A.A.

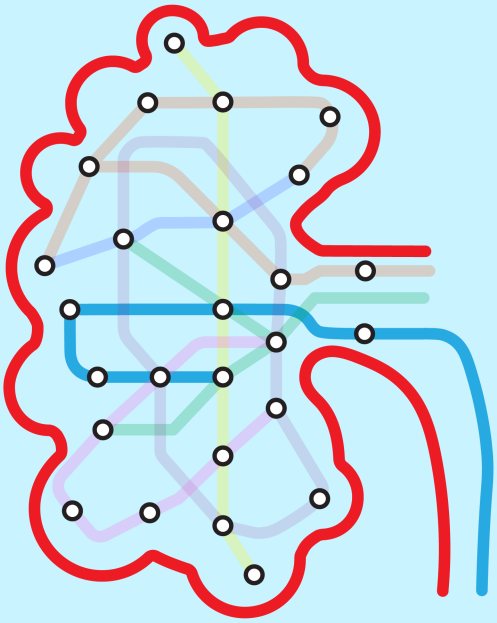

CHAPTER 6

Fiboflapon reduces cyst swelling *in vitro*, but does not affect cyst growth *in vivo*

Anish A. Kanhai[1], Hester Bange[2], Tareq B. Malas[1], Romy Ramdjan[1], Leo S. Price[2], Gerard J.P. van Westen[3], Peter A.C. 't Hoen[1,4], Wouter N. Leonhard[1], Dorien J.M. Peters[1]

[1]Department of Human Genetics, Leiden University Medical Center, The Netherlands

[2]CrownBio Netherlands B.V., Leiden, the Netherlands

[3]Drug Discovery and Safety, Leiden Academic Centre for Drug Research, Leiden, The Netherlands

[4]Center for Molecular and Biomolecular Informatics, Radboud Institute for Molecular Life Sciences, Radboud University Medical Center Nijmegen, Nijmegen, the Netherlands

Manuscript

Abstract

With costs for modern drug discovery and development reaching up to $ 3 billion per drug, strategies for drug repurposing are gaining more interest as a more affordable alternative to repurpose existing drugs for novel indications. An indication that could very well benefit from this approach is autosomal dominant polycystic kidney disease (ADPKD), the most common genetic kidney disease affecting 1 in 1000-2500 individuals worldwide. As a platitude of dysregulated signalling pathways are underlying ADPKD disease progression, there are likely multiple approved drugs on the market that could inhibit cyst growth and reduce disease progression. Utilizing novel approaches in gene expression profiling, bioinformatics and cheminformatics, we previously showed that market-approved drugs can be linked to genes and proteins dysregulated in ADPKD. Here, we focused on the best performing drug of our previous screening, the 5-lipoxygenase activating protein antagonist fiboflapon. We found fiboflapon to reduce 3D cyst swelling in both murine and human cultures, without inducing cell toxicity. However, in a progressive, early-onset mouse model for ADPKD, we found fiboflapon to be ineffective in inhibiting cyst growth and reducing cyst progression.

Introduction

In the modern drug discovery and development landscape, the costs for developing a novel drug from scratch are exorbitantly high, with recent studies estimating the costs around $ 1-3 billion[1,2]. As only a small amount of drug candidates are accepted for patient treatment, limiting its cost-benefit ratio, a new strategy that has emerged in recent years for the identification of new drugs is drug repurposing. Defined as the application of known drugs and compounds to treat new indications, drug repurposing can save a substantial amount of costs in (pre)clinical research, as a reduced amount of experiments and trials is necessary for regulatory approval[3]. In addition, production lines are already in place, further lowering costs. Moreover, predicting and validating new targets for existing drugs and compounds is easier now due to computational and biological analysis advancements, making drug repurposing an even more viable strategy[4,5]. The most popular example of drug repurposing is the use of sildenafil (Viagra©) for the treatment of erectile dysfunction, while originally developed for the treatment of hypertension[6,7]. More recently, the COVID-19 pandemic prompted a large amount of drug repurposing studies, resulting in the antiviral drug remdesivir now named a first-in-class medication by the FDA for COVID-19 treatment[8-14].

Another disease well suited for drug repurposing strategies is autosomal dominant polycystic kidney disease (ADPKD). Affecting around 1 in 1000 to 2500 individuals, it is the most common genetic renal condition[15]. The main causes are mutations in either the *PKD1* or *PKD2* genes, encoding polycystin-1 (PC-1) and polycystin-2 (PC-2), respectively[16,17]. Due to these mutations, fluid-filled cysts develop in the kidney, increasing in both number and size over time, ultimately resulting in end-stage renal disease (ESRD)[18]. This decline is partly due to a massive dysregulation of intracellular signalling pathways, which are (in)directly regulated by the polycystin proteins. Due to the dysregulation, ADPKD can be characterized by excessive cell proliferation, Warburg-like metabolic reprogramming as well as increases in fluid secretion, inflammation and fibrosis[15]. The only treatment option approved so far by regulatory agencies is the vasopressin V2 receptor tolvaptan, which slows down kidney growth and reduces kidney function decline[19,20]. However, serious side effects, including polyuria and hepatotoxicity, have limited tolvaptan use to a small subset of ADPKD patients. A large amount of (pre)clinical studies has been performed or is currently underway, but none have resulted in an approved treatment thus far[21]. Therefore, a large clinical need remains unmet.

Due to the large and quick developments in genetic sequencing techniques, new avenues of research have opened up that utilize these methods to find associations between genes and diseases, for example as a risk factor or druggable target[22-25]. In the context of drug repurposing, large-scale perturbation databases, such as the Connectivity Map

or Library of Integrated Network-based Cellular Signatures (LINCS), provide the scientific community with transcriptional profiles of cell lines treated with a plethora of chemical compounds, to serve as a reference[26-28]. These databases have already been used in search for possible drug repurposing targets in ADPKD[29,30]. Our group recently showed that in a more integrative computational approach, combining gene expression profiling, bioinformatics, and cheminformatics, compounds can be identified that are linked to genes and proteins dysregulated in ADPKD and that are effective in reducing cyst growth *in vitro*[31]. Out of these hits, the 5-lipoxygenase activating protein (FLAP) inhibitor fiboflapon showed the most promise. FLAP is part of the leukotriene synthesis pathway, in which free arachidonic acid is metabolized to leukotriene B_4 (LTB_4), leukotriene C_4 or lipoxin A_4 through multiple intermediate steps (Figure 1). FLAP, also known as arachidonate 5-lipoxygenase activating protein (ALOX5-AP), is responsible for 5-lipoxygenase (ALOX5) activation, which in turn catalyzes the conversion of arachidonic acid to 5-hydroperoxyeicosatetraenoic acid (5-HpETE) to leukotriene A_4, the first steps of the leukotriene synthesis pathway. In this study, we continue on our previous findings, and find the FLAP inhibitor fiboflapon to be effective in reducing cyst growth in both murine and human 3D ADPKD cultures, but not in a progressive, early-onset ADPKD mouse model.

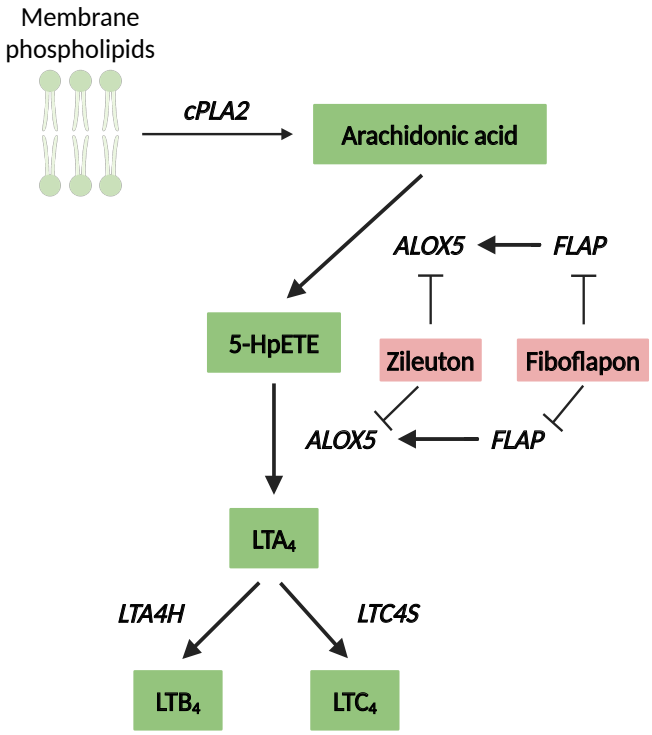

Figure 1: The leukotriene synthesis pathway
Through hydrolysis, cytosolic phospholipase A_2 (cPLA2) releases arachidonic acid from membrane phospholipids.
Free arachidonic acid is then transferred by 5-lipoxygenase activating protein (FLAP, also called ALOX5-AP) to the 5-lipoxygenase (ALOX5) enzyme, simultaneously activating the latter. ALOX5 then metabolizes arachidonic acid to 5-hydroperoxyeicosatetraenoic acid (5-HpETE), which is quickly converted to leukotriene A_4 (LTA_4) by the FLAP/ALOX5 enzyme complex. LTA_4 hydrolase (LTA4H) and leukotriene C_4 synthase (LTC4S) can then convert LTA_4 to leukotriene B_4 (LTB_4) or leukotriene C_4 (LTC_4), respectively. Leukotriene synthesis can be inhibited by the FLAP inhibitor fiboflapon, as well as the ALOX5 inhibitor zileuton. Figure created with BioRender.

Material & Methods

mIMCD3 3D cyst model

mIMCD3 3D cyst cell culture and compound treatments were performed as described before[32]. In short, mIMCD3 *Pkd1*$^{-/-}$ (mIMRFNPKD 5E4) cells were expanded in cell culture medium (DMEM/F12 (Ham's) culture medium (D8062, Sigma-Aldrich), supplemented with 10% fetal bovine serum (FBS, F7524, Sigma-Aldrich), GlutaMAX™ (35050038, Gibco, Life Technologies), and penicillin/streptomycin (15140122, Gibco, Life Technologies)) for 72 hours. Cells were then washed with 1x phosphate-buffered saline (PBS), trypsinized with 1x trypsin-EDTA (T4174, Sigma-Aldrich) and mixed with Cyst-Gel (CrownBio Netherlands) to a final concentration of 150000 cells/mL. The cell-gel mixture was then pipetted to 384-well plates (Greiner Clear, Greiner Bio-One B.V.) using Cybi Felix robotic liquid handler (Analytic Jena AG). After polymerization of the gel, cell culture medium was added. Cells were allowed to form cysts for 96 hours, after which cysts were exposed to vehicle (0.2% DMSO), 2.5 µM forskolin (34427, Calbiochem, Millipore B.V.), fiboflapon (HY-15874A, MedChemExpress) and/or zileuton (10006967, Cayman Chemical) for 72 hours. Afterwards, cysts were fixed with 4% formaldehyde (Sigma-Aldrich) and simultaneously permeabilized with 0.2% Triton-X100 (Sigma-Aldrich) and stained with 0.25 M rhodamine-phalloidin (Sigma-Aldrich) and 0.1% Hoechst 33258 (Sigma-Aldrich) in 1x PBS for 12 hours at 4 °C in the dark. Imaging was done using the Molecular Devices ImageXpress Micro XLS (Molecular Devices) with a 4x NIKON objective. For both channels, between 30–35 images throughout the entire z-stack were made for each well, 50 µm apart. Each individual image was analysed using Ominer™ image analysis software (CrownBio Netherlands) integrated in KNIME Analytics platform (http://www.knime.org/). The automated calculation of various phenotypic characteristics related to cyst area and cytotoxicity was performed as described before[32].

Human ADPKD 3D cyst model

The human ADPKD 3D cyst assay was performed as described before[33]. In short, human renal cells were obtained via ADPKD patient nephrectomy (*PKD1* mutation: c.5622G>A p.Trp1874∗; kindly provided by the Leiden University Medical Center). Cells were mixed with PrimCyst-Gel (CrownBio Netherlands) and the mixture was then pipetted to 384-well plates to a final cell density of 450 cell clusters/well. After gel polymerization, cell culture medium was added. Cells were grown in the gel matrix for 24 hours, after which newly formed cysts were exposed to vehicle (0.2% DMSO + PBS), 2.5 µM forskolin to induce cyst swelling, fiboflapon and/or zileuton for 48 hours. Cysts were fixed with 4% formaldehyde (Sigma-Aldrich), permeabilized with 0.2% Triton X-100 (Sigma-Aldrich), and stained with 0.25 µM rhodamine-phalloidin (Sigma-Aldrich) and 0.1% Hoechst 33258 (Sigma-Aldrich) for 2 days. Imaging was done using ImageXpress Micro XLS (Molecular Devices). For each well, approximately 35 images in the Z- direction were made for both channels, capturing the

whole z plane for the whole well in each image. Image analysis was performed using Ominer software (CrownBio Netherlands). The automated calculation of cyst area and cytotoxicity was performed as previously described[32].

Mouse experimental studies

Generation of tamoxifen-inducible kidney-specific Pkd1 deletion (iKspCre-*Pkd1*^{del}) mice (tam-*KspCad*-CreER^{T2}; *Pkd1*$^{del2\text{-}1L/lox2\text{-}11}$) was done in-house, as described before[34,35]. All animal experiments were approved by the Animal Experiment Ethics Committee of Leiden University Medical Center and the Commission Biotechnology in Animals of the Dutch Ministry of Agriculture, and performed in accordance to Directive 2010/63/EU for animal experiments. iKspCre-*Pkd1*^{del} mice were generated (n = 7-8 mice for wildtype groups, n = 13-14 mice for cystic groups) and kidney-specific deletion of the *Pkd1* gene was induced by administration of 150 mg/kg tamoxifen (T5648, Sigma-Aldrich) via oral gavage on postnatal day (PN) 10 & 11. On PN13, treatment was started with either 3 mg/kg or 10 mg/kg fiboflapon (dissolved in DMSO) via daily oral gavage in 0.5% methylcellulose solution. The vehicle group received the same DMSO concentration in 0.5% methylcellulose solution via daily oral gavage. At PN28, blood samples were taken for plasma measurements and blood urea nitrogen (BUN) measurements using the Reflotron Sprint (Roche Diagnostics), after which mice from all groups were sacrificed. Kidneys were then removed, weighed, bisected and either snap-frozen in liquid nitrogen or fixed in 4% buffered paraformaldehyde. Snap-frozen tissues were stored at -80 °C until further use.

Histology and immunohistochemistry

Tissues fixed overnight in 4% buffered formaldehyde were embedded in paraffin. Sections were stained with Periodic acid-Schiff (PAS) and Sirius Red (SR) using standard protocols. Cystic and fibrotic indices were calculated as previously described[36-38]. Specific color pallets were designed with Photoshop software (Adobe Systems Inc.). F4/80 stainings were performed to detect macrophages. Antigen retrieval was done with proteinase K (Dako), followed by endogenous peroxide blocking by 20 min. incubation with 0.12% H_2O_2. Tissue sections were then incubated with rat anti-F4/80 (Serotec) and a secondary incubation with anti-rat IMMPress (MP-7444, Vectorlabs). Immune reactions were revealed using diaminobenzidine as a chromogen and counterstained with hematoxylin. Sections were then dehydrated, mounted and quantified with Photoshop software (Adobe) as described before[36].

Plasma LTB_4 measurements

Blood samples were drawn from mice (PN28) before sacrifice in heparin-coated capillaries (Microvette® CB 300 LH, Sarstedt). Sample work-up was done as described before[39]. 0.75 mM A23187 (C7522, Sigma-Aldrich) was added to induce LTB_4 production in blood cells,

samples were incubated at 37 °C for 30 min. and then centrifuged at 300 *x g* for 10 min. at 4 °C[40]. Plasma was then isolated and stored at -80 °C until further use. Plasma LTB_4 concentrations were determined with an immunoassay (KGE006B, R&D Systems) according to manufacturer's instructions.

Statistical analyses

Statistical & data analyses were performed with GraphPad Prism 8 (GraphPad Software). All results are expressed as mean ± SD, unless stated otherwise in the figure legends. Comparisons between two groups were done using the two-tailed unpaired Student's t test (normal distributed data) or the Mann-Whitney U-test (non-normal distributed data), while comparisons between multiple groups were done using the one-way ANOVA, followed by Tukey's or Dunnett's multiple comparison test. Results were considered statistically significant when $p < 0.05$ or FDR <0.05. *$p < 0.05$, **$p < 0.01$, ***$p < 0.001$, ****$p < 0.0001$.

Results

Fiboflapon reduces cyst swelling in mouse and human renal 3D cysts

Previous results based on comprehensive gene expression profiling combined with bioinformatics and cheminformatics indicated that the FLAP inhibitor fiboflapon could potentially inhibit cyst growth and disease progression in ADPKD[31]. To investigate this, we first tested fiboflapon's capacity to inhibit and reduce cyst swelling in our mouse 3D cyst swelling assay[32]. mIMCD3 *Pkd1*$^{-/-}$ cells were grown in an extracellular matrix-based hydrogel and cyst swelling was induced by addition of 2.5 µM forskolin for 72 hours. To test fiboflapon, cells were co-incubated with forskolin and increasing concentrations of fiboflapon (0.1 – 40 µM) for 72 hours. Calculation of the cyst area showed that fiboflapon can reduce cyst swelling in this assay in a dose-dependent manner, without exhibiting toxic effects (Figure 2A-B). To investigate the involvement of ALOX5 (the target of FLAP) in this process, we also tested the ALOX5 inhibitor zileuton in increasing concentrations (0.1 – 100 µM) in this assay. However, zileuton did not reduce cyst swelling in this assay, as demonstrated before, and shows that the cyst swelling reduction induced by fiboflapon is ALOX5-independent (Figure 2A)[31].

We also tested fiboflapon in ADPKD patient cells obtained post-nephrectomy. These patient-derived cells are grown in an extracellular matrix hydrogel (PrimCyst-Gel) for 24 hours and are subsequently treated with 2.5 µM forskolin for 48 hours to induce cyst swelling. To test fiboflapon, cells were co-incubated with increasing concentrations of fiboflapon (0.1 – 100 µM) for 48 hours. Zileuton (0.1 – 100 µM) was again included to evaluate ALOX5 dependency. Cyst area calculations show that fiboflapon reduces cyst swelling in ADPKD patient-derived cells in a dose-dependent and non-toxic manner, while zileuton treatment has no effect on these cells (Figure 2C-D). These results are in line with the mouse 3D cyst swelling assay and confirm that fiboflapon is a viable candidate for further investigation as a potential ADPKD treatment.

Fiboflapon does not affect renal health or cyst growth in a progressive, early-onset ADPKD mouse model

We continued our investigation into fiboflapon's potential as an ADPKD treatment by testing fiboflapon in a early-onset, tamoxifen-inducible, conditional *Pkd1* deletion mouse model[34,35]. This model is characterized by rapid cyst formation in virtually all segments of the kidneys after gene disruption, reaching renal failure after approximately 20 days post-induction. *Pkd1* deletion in mice was induced by tamoxifen administration at PN day 10 & 11, after which daily fiboflapon administration via oral gavage started on PN 13 until PN 28 (Figure 3A). Based on previously published preclinical studies with fiboflapon in rat models, we opted to test a low dose (3 mg/kg body weight) and a high dose (10 mg/kg body weight)

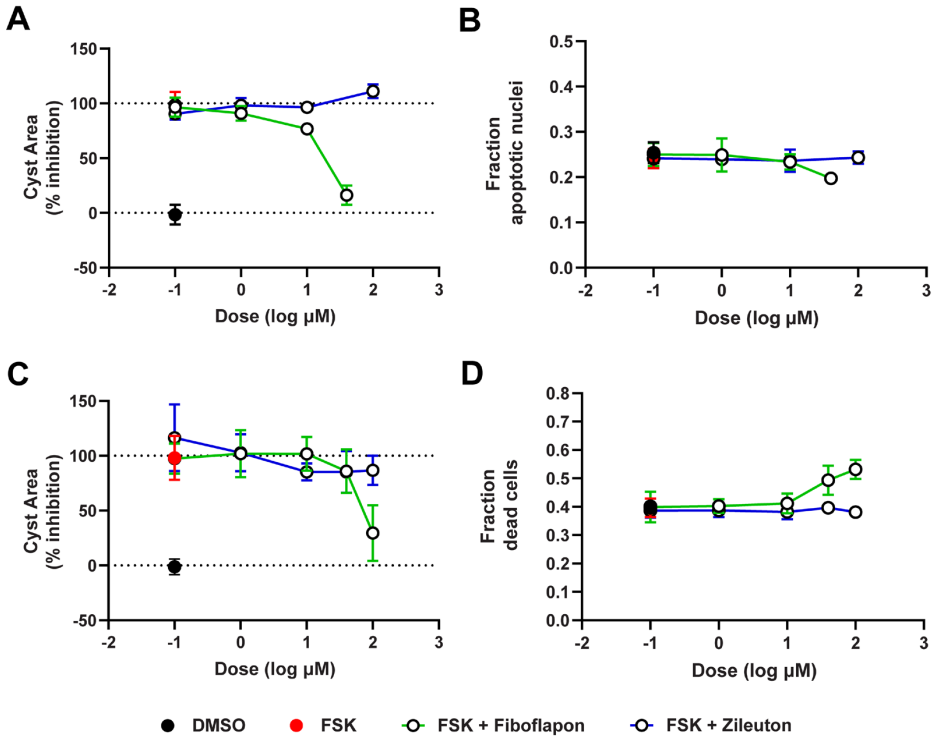

Figure 2: Fiboflapon reduces 3D cyst swelling in both murine and ADPKD patient-derived 3D cultures

(A) Cyst area (presented as % inhibition compared to unstimulated vehicle control) of mIMCD3 *Pkd1*$^{-/-}$ cysts treated with forskolin and fiboflapon (green) or zileuton (blue). Dotted line at 0% represents unstimulated vehicle control, dotted line at 100% represents stimulated control (2.5 µM forskolin). **(B)** Fraction of apoptotic nuclei of mIMCD3 *Pkd1*$^{-/-}$ cysts treated with forskolin and fiboflapon (green) or zileuton (blue) for 72h. Cell death was calculated by automatic calculation of various phenotypic characteristics as described before (see Methods section). **(C)** Cyst area (presented as % inhibition compared to unstimulated vehicle control) of 3D-cultured human ADPKD patient-derived kidney cells treated with forskolin and fiboflapon (green) or zileuton (blue) for 48h. Dotted line at 0% represents unstimulated vehicle control, dotted line at 100% represents stimulated control (2.5 µM forskolin). **(D)** Fraction of dead cells of human ADPKD patient-derived kidney cells treated with forskolin and fiboflapon (green) or zileuton (blue) for 48h. Cell death was calculated by automatic calculation of various phenotypic characteristics as described before (see Methods section). Each dot represents the average of 4 replicates per condition.

fiboflapon treatment[39]. No differences in body weight development were observed between non-treated and treated animals, both for wildtype and *Pkd1* deletion mice, indicating that fiboflapon treatment was not toxic (Figure 3B). *Pkd1* deletion induced a marked increase in 2-kidney weight to body weight ratio (2KW/BW), but this was unaffected by both low and high dose fiboflapon administration.(Figure 3C). In addition, blood urea nitrogen levels in *Pkd1* deletion mice were also unaffected by fiboflapon treatment (Figure 3D). These data suggest that fiboflapon cannot slow disease progression in a progressive, early-onset ADPKD mouse model.

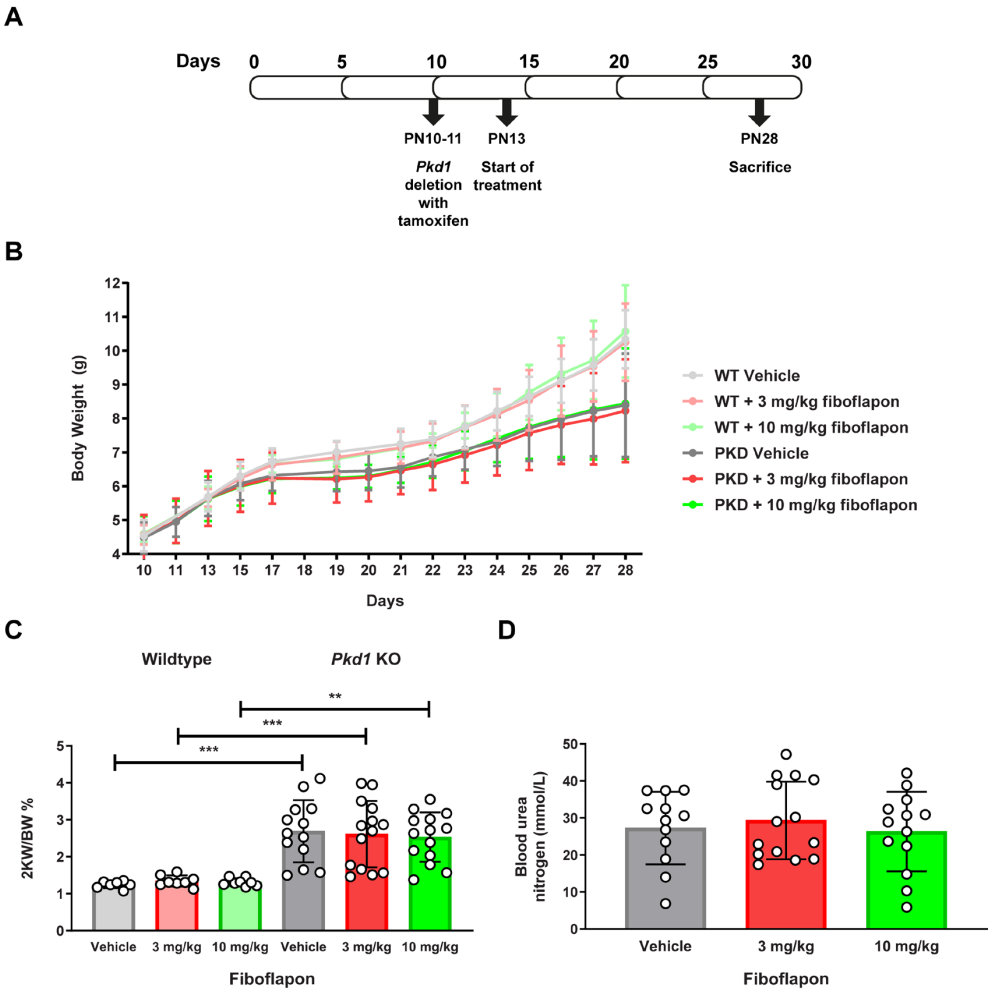

Figure 3: Fiboflapon does not affect renal health or cyst growth in a progressive, early-onset PKD mouse model

(A) Graphical representation of the preclinical study. Tamoxifen (150 mg/kg) was administered to mice on PN10 & 11 to delete *Pkd1*. Treatments started at PN13 and continued until PN28, at which point the experiment was ended. **(B)** Body weight (g) development of wildtype (light colors) or tamoxifen-induced *Pkd1*$^{-/-}$ mice (dark colors) treated with vehicle (grey), 3 mg/kg/day fiboflapon (red) or 10 mg/kg/day fiboflapon (green). **(C)** 2KW/BW% of wildtype (light colors) or tamoxifen-induced *Pkd1*$^{-/-}$ mice (dark colors) treated with vehicle (grey), 3 mg/kg/day fiboflapon (red) or 10 mg/kg/day fiboflapon (green) at the end of the experiment. **(D)** Blood urea nitrogen levels (mmol/L) of tamoxifen-induced *Pkd1*$^{-/-}$ mice treated with vehicle (grey), 3 mg/kg/day fiboflapon (red) or 10 mg/kg/day fiboflapon (green). Results are expressed as mean ± SD, each dot represents a mouse. **P<0.01, ***P<0.001, measured by two-tailed unpaired Student's *t*-test. PN: post-natal, WT = wildtype, KO = knock-out, 2KW/BW% = 2-kidney weight-to-body weight-percentage.

Renal fibrosis and macrophage infiltration are not affected by fiboflapon treatment in cystic kidneys

To confirm our findings, we performed immunohistochemical analysis on kidneys obtained from the study. Induction of *Pkd1* deletion by tamoxifen administration resulted in increased cystic disease severity, resulting in a higher cystic index (Figure 4, 5A). Both general renal histology and the cystic index are unaffected by fiboflapon treatment compared to cystic mice (Figure 4, 5A). As one of the hallmarks of ADPKD is increased renal fibrosis due to

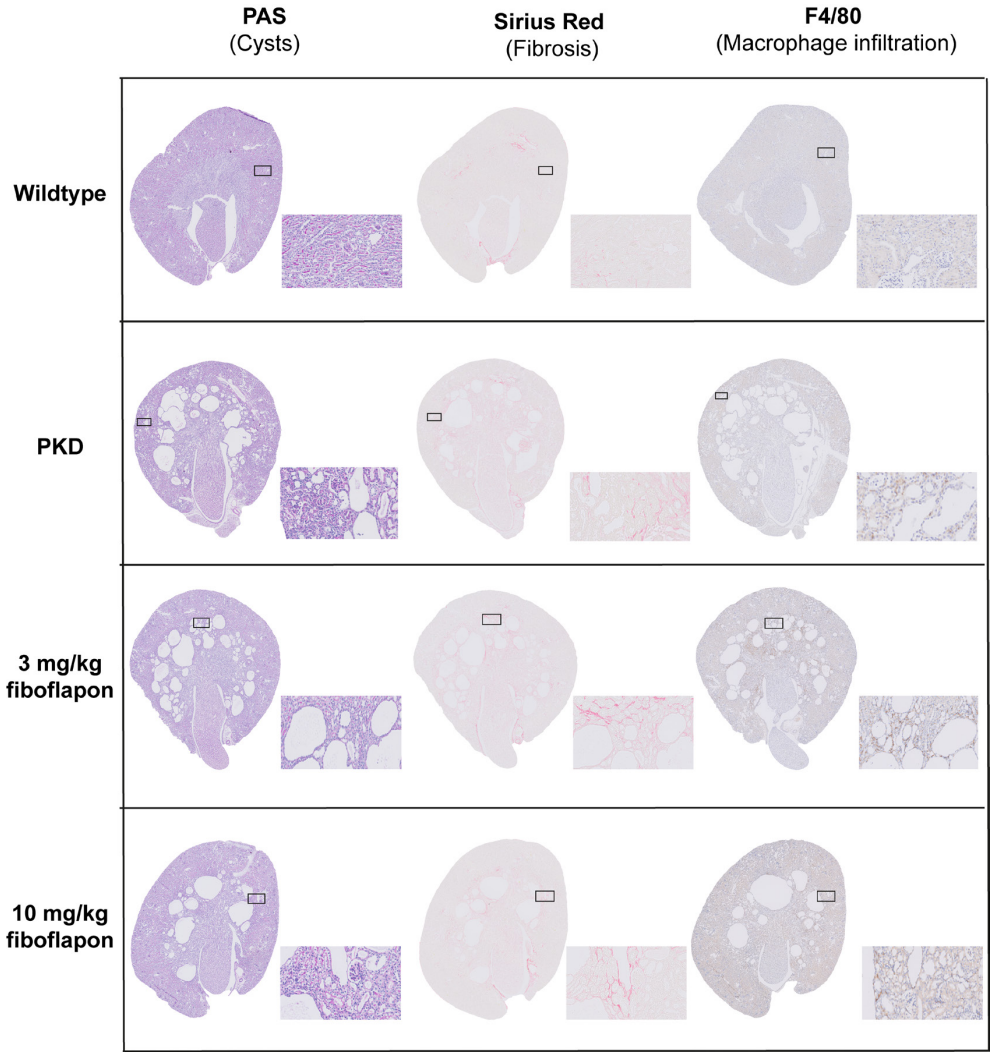

Figure 4: Fiboflapon does not affect disease severity, renal fibrosis or macrophage infiltration in cystic kidneys

Representative image of PAS-, Sirius Red and F4/80-stained kidney sections from each treatment group. *Pkd1* deletion with tamoxifen increases cystic disease severity, renal fibrosis and macrophage infiltration, while both 3 mg/kg and 10 mg/kg fiboflapon treatment do not affect this.

inflammatory signalling, we also analyzed the level of renal fibrosis via Sirius Red staining. We observed a similar pattern for fibrosis development, i.e. increased fibrosis upon *Pkd1* deletion, although non-significant, and no change with fiboflapon treatment compared to cystic mice (Figure 4, 5B). The infiltration of macrophages into the cystic kidney is closely related to promoting inflammation and the development of renal fibrosis. Therefore, we investigated the amount of macrophages present by staining for the macrophage marker F4/80. Again, we observed a similar pattern, i.e. an increased amount of macrophages in cystic kidneys, and no change with fiboflapon compared to cystic mice (Figure 4, 5C). These data further reinforce the suggestion that fiboflapon does not affect disease progression in a early-onset ADPKD mouse model, and that important disease mechanisms such as fibrosis and macrophage accumulation are also unaffected by fiboflapon.

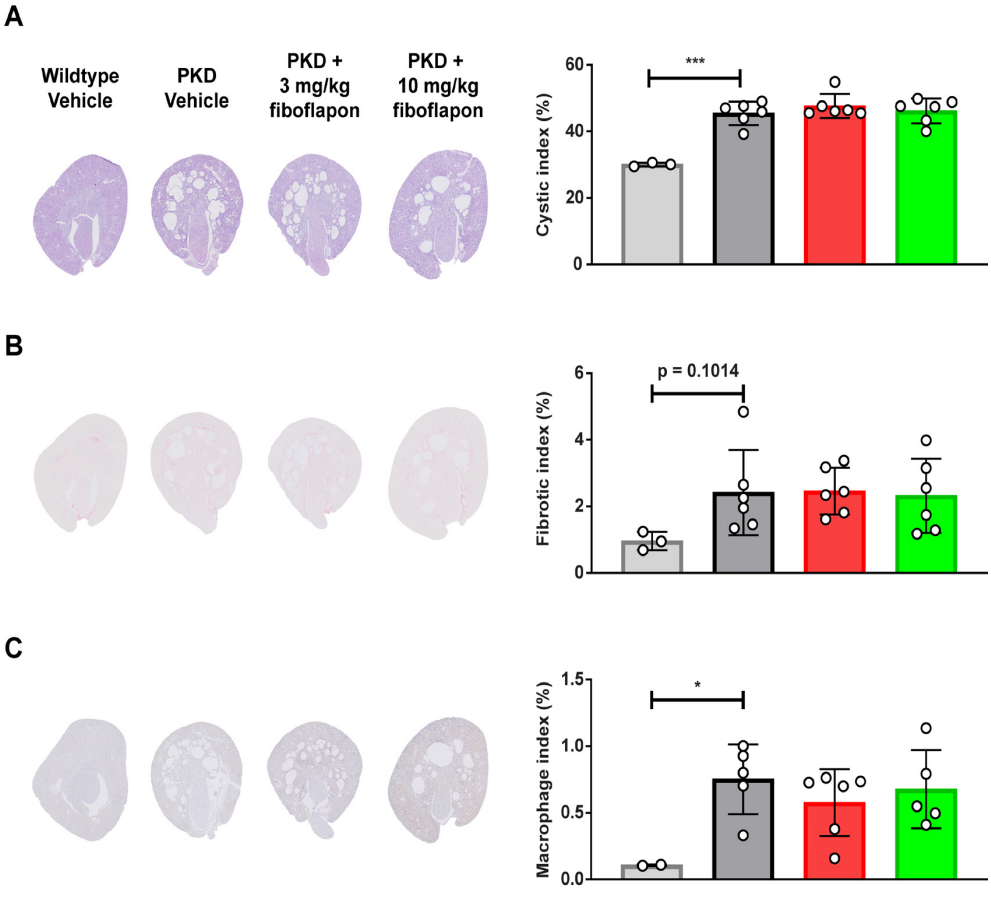

← Figure 5: Fiboflapon does not affect the cystic, fibrotic or macrophage index in cystic kidneys

(A) Representative images of PAS-stained kidney sections from each treatment group and corresponding quantification of the cystic index (represented as % cystic area of total tissue). For each group, the image corresponding to the median 2KW/BW% is shown. **(B)** Representative images of Sirius Red-stained kidney sections of each treatment group and corresponding quantification of the fibrotic index (represented as % Sirius Red positive pixels of total pixels). For each group, the image corresponding to the median 2KW/BW% is shown. **(C)** Representative images of F4/80-stained kidney sections of each treatment group and corresponding quantification of the macrophage index (represented as % F4/80 positive pixels of total pixels). For each group, the image corresponding to the median 2KW/BW% is shown. Results are expressed as mean ± SD, each dot represents a mouse. *P<0.05, ***P<0.001, measured by two-tailed unpaired Student's *t*-test.

Fiboflapon affects leukotriene synthesis in blood cells

The observed inefficacy of fiboflapon on cyst growth and renal health could be due to a systemic lack of compound uptake. To verify whether this was the case, we measured leukotriene B4 (LTB_4) levels in plasma samples of untreated wildtype mice and of wildtype mice treated with 10 mg/kg fiboflapon for a similar duration to our mouse study. LTB_4 is one of the end products of the leukotriene synthesis pathway, which starts with arachidonic acid conversion, in part regulated by FLAP. We found plasma LTB_4 levels to be significantly reduced by fiboflapon treatment (Figure 6). This shows that a systemic lack of compound uptake is unlikely to be behind the observed inefficacy of fiboflapon.

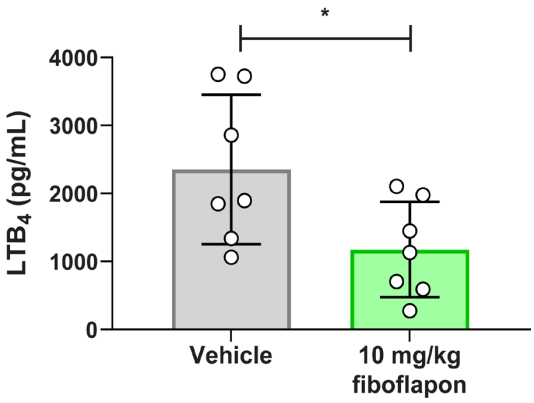

Figure 6: Plasma LTB_4 levels are reduced by fiboflapon treatment in wildtype mice

Plasma LTB_4 concentrations (pg/ml) of wildtype mice treated with vehicle (grey) or 10 mg/kg/day fiboflapon (green). Results are expressed as mean ± SD, each dot represents a mouse. *P<0.05, measured by two-tailed Student's *t*-test. LTB_4 = leukotriene B4.

Discussion

ADPKD is currently the most prevalent genetic kidney disease and the fourth most common disease requiring renal replacement therapy, accounting for approximately 10%[15,41]. As a large portion of ADPKD patients cannot use the only currently approved treatment tolvaptan, in part due to its side effects, there is a large, unmet need for new therapeutics. Drug repurposing has emerged as a viable research strategy in identifying such therapeutics, in part due to financial and regulatory benefits as well as technological advancements. By combining transcriptomics, bioinformatics and cheminformatics, we previously identified several targets of interest, dysregulated in ADPKD and tested multiple compounds for those targets. These compounds were effective in reducing cyst growth *in vitro*, showing this analysis is effective in identifying novel ADPKD therapeutics[31]. We here present follow-up research on one hit compound, the FLAP inhibitor fiboflapon, which we found to be effective in reducing cyst growth *in vitro*, but did not affect cyst growth in a progressive, early-onset ADPKD mouse model.

FLAP activates ALOX5 and by extension, pro-inflammatory mediator production via the leukotriene synthesis pathway, by transfer of free arachidonic acid to ALOX5 (Figure 1)[42]. Therefore, we anticipated any effects of fiboflapon to be mediated via the leukotriene synthesis pathway. However, we observed *in vitro* in both murine and human 3D cyst assays that zileuton, an inhibitor of ALOX5, did not inhibit 3D cyst growth, while fiboflapon did inhibit 3D cyst growth. This discrepancy suggests that the positive effects of fiboflapon *in vitro* are not mediated through ALOX5 and the leukotriene synthesis pathway. This is further emphasized by the lack of immune cells in the 3D cyst assays, while leukotriene synthesis mainly occurs in leukocytes, in particular neutrophils and macrophages[43-45]. This points to possible secondary targets that are targeted by fiboflapon or FLAP. However, preclinical data on fiboflapon is scarce, making further speculation on this challenging. In contrast, proteomics on human tissues have found multiple FLAP binding partners, unrelated to leukotriene synthesis[46,47]. While numerous binding partners have been found in these studies, those of note are the chloride intracellular channel 1 (CLIC1), aquaporin-6 (AQP6) and free fatty acid receptor 2 (FFRA2). All can be linked directly to molecular mechanisms involved in ADPKD pathogenesis, namely fluid secretion into the cyst lumen, driven by chloride secretion and water transport, and dysregulated energy metabolism, of which altered fatty acid metabolism is a part[48,49]. By inhibiting FLAP, fiboflapon could potentially inhibit these processes as well, but further studies are needed to validate these hypotheses.

Other discrepancies between the inhibitory effects of fiboflapon and zileuton are found *in vivo*. While we observe no effects of fiboflapon on disease progression in our progressive, early-onset PKD mouse model, a previous study has shown that ALOX5 inhibition by zileuton

reduces renal fibrosis, but not cell proliferation and immune cell infiltration, in an unilateral ureteral obstruction (UUO) model, a disease model with many overlaps with PKD in regards to the disease mechanisms involved[50]. In ADPKD pathogenesis, abnormal immune response is an important driver of disease progression[15]. Leukotriene synthesis mainly occurs in neutrophils and macrophages[43-45]. While the role of neutrophils in ADPKD pathogenesis is limited, macrophages are known to promote disease progression[15,51,52]. Indeed, we show an increased macrophage presence in the cystic kidney, unaffected by fiboflapon treatment (Figure 4C). This is in line with the UUO model, which also showed increased macrophage infiltration, unaffected by zileuton treatment[50]. However, while zileuton does improve renal health after UUO due to reduced renal fibrosis, we do not observe such an effect after fiboflapon treatment (Figure 4B)[50]. The disparity in the results could be explained by differences in contribution of those mechanisms to the overall disease progression. In our progressive PKD model, disease progression appears to be more dependent on increased cell proliferation, while in the adult UUO model, alterations in cellular metabolism and an increased inflammatory response are contributing more[53,54]. As leukotriene synthesis is mainly occurring in immune cells , it follows that in an environment in which proliferative pathways are more dominant over pro-inflammatory pathways, leukotriene synthesis inhibition is less effective, which is what we observe.

Another factor in the disparity in results between zileuton and fiboflapon is the developmental status of the models used. We tested fiboflapon in a early-onset young PKD mouse model, while zileuton was tested in an adult UUO model. The PKD mouse model is highly progressive, with renal failure reached within a month after *Pkd1* deletion. While results can be generated fast in this model, it might also mean that due to the high rate of disease progression, it is not feasible for potential therapeutics to show efficacy, as their effects are overpowered by the rate of disease progression. A slower progressive model, in which ADPKD disease progression is better mimicked, should therefore be more suited to test preclinical efficacy.

Other than the model used, the lack of fiboflapon efficacy *in vivo* could also be attributed to the lack of compound uptake into the kidney. Although we observe systemic effects of fiboflapon efficacy by lowered plasma LTB_4 concentrations, we did not test whether this is also the case in kidneys. While no data is available on fiboflapon and its potential uptake in the kidney, insufficient uptake into the kidney could be behind the lack of fiboflapon efficacy. With public preclinical reports on fiboflapon only scarcely available, we based our dosages for this study on the reports available and tested doses of 3 mg/kg and 10 mg/kg in our mouse model[39]. However, several phase 1 and phase 2 clinical investigations using fiboflapon in respiratory conditions are also available[55-60]. Interconversions between human dosages and rodent dosages are possible by correcting not just for the body weight, but also

body length and the human equivalent dose[61]. Interconversion of the human study doses which include multi-day treatment to an equivalent dose for mice yields a range of 15-30 mg/kg/day. This is 1.5 to 3 times higher than the highest dose we used based on preclinical reports. Therefore, future studies on the therapeutic effect of fiboflapon in ADPKD should use a slower progressive model, more representative of human disease progression as well as a higher dosage, better suited to the human equivalent dosage. In addition, fiboflapon uptake into the kidney should be evaluated.

In conclusion, our drug repurposing strategy combining transcriptomics, bioinformatics and cheminformatics yielded the FLAP inhibitor fiboflapon, which was effective in inhibiting 3D cyst swelling in both mouse and patient-derived tissues. However, fiboflapon was not able to inhibit disease progression in a early-onset, tamoxifen-inducible, conditional *Pkd1* deletion mouse model. Moreover, fiboflapon did not alter disease-induced changes in renal health, cystic severity, renal fibrosis and macrophage infiltration. Due to the chosen PKD mouse model and fiboflapon dose, we cannot conclude with certainty fiboflapon is ineffective in ADPKD. Future studies in a slowly progressive PKD mouse model, more relevant to human disease, a re-evaluation of the fiboflapon dose used in such studies, as well as validation of renal fiboflapon uptake will answer whether fiboflapon can be a future therapeutic candidate in ADPKD.

References

1. DiMasi, J.A., Grabowski, H.G., and Hansen, R.W. (2016). Innovation in the pharmaceutical industry: New estimates of R&D costs. Journal of Health Economics *47*, 20-33. https://doi.org/10.1016/j.jhealeco.2016.01.012.

2. Wouters, O.J., McKee, M., and Luyten, J. (2020). Estimated Research and Development Investment Needed to Bring a New Medicine to Market, 2009-2018. Jama *323*, 844-853. 10.1001/jama.2020.1166.

3. Ashburn, T.T., and Thor, K.B. (2004). Drug repositioning: identifying and developing new uses for existing drugs. Nature Reviews Drug Discovery *3*, 673-683. 10.1038/nrd1468.

4. Campillos, M., Kuhn, M., Gavin, A.C., Jensen, L.J., and Bork, P. (2008). Drug target identification using side-effect similarity. Science *321*, 263-266. 10.1126/science.1158140.

5. Keiser, M.J., Setola, V., Irwin, J.J., Laggner, C., Abbas, A.I., Hufeisen, S.J., Jensen, N.H., Kuijer, M.B., Matos, R.C., Tran, T.B., et al. (2009). Predicting new molecular targets for known drugs. Nature *462*, 175-181. 10.1038/nature08506.

6. Terrett, N.K., Bell, A.S., Brown, D., and Ellis, P. (1996). Sildenafil (VIAGRATM), a potent and selective inhibitor of type 5 cGMP phosphodiesterase with utility for the treatment of male erectile dysfunction. Bioorganic & Medicinal Chemistry Letters *6*, 1819-1824. https://doi.org/10.1016/0960-894X(96)00323-X.

7. Boolell, M., Allen, M.J., Ballard, S.A., Gepi-Attee, S., Muirhead, G.J., Naylor, A.M., Osterloh, I.H., and Gingell, C. (1996). Sildenafil: an orally active type 5 cyclic GMP-specific phosphodiesterase inhibitor for the treatment of penile erectile dysfunction. Int J Impot Res *8*, 47-52.

8. Warren, T.K., Jordan, R., Lo, M.K., Ray, A.S., Mackman, R.L., Soloveva, V., Siegel, D., Perron, M., Bannister, R., Hui, H.C., et al. (2016). Therapeutic efficacy of the small molecule GS-5734 against Ebola virus in rhesus monkeys. Nature *531*, 381-385. 10.1038/nature17180.

9. Sheahan, T.P., Sims, A.C., Graham, R.L., Menachery, V.D., Gralinski, L.E., Case, J.B., Leist, S.R., Pyrc, K., Feng, J.Y., Trantcheva, I., et al. (2017). Broad-spectrum antiviral GS-5734 inhibits both epidemic and zoonotic coronaviruses. Sci Transl Med *9*. 10.1126/scitranslmed.aal3653.

10. Brown, A.J., Won, J.J., Graham, R.L., Dinnon, K.H., 3rd, Sims, A.C., Feng, J.Y., Cihlar, T., Denison, M.R., Baric, R.S., and Sheahan, T.P. (2019). Broad spectrum antiviral remdesivir inhibits human endemic and zoonotic deltacoronaviruses with a highly divergent RNA dependent RNA polymerase. Antiviral Res *169*, 104541. 10.1016/j.antiviral.2019.104541.

11. Sheahan, T.P., Sims, A.C., Leist, S.R., Schäfer, A., Won, J., Brown, A.J., Montgomery, S.A., Hogg, A., Babusis, D., Clarke, M.O., et al. (2020). Comparative therapeutic efficacy of remdesivir and combination lopinavir, ritonavir, and interferon beta against MERS-CoV. Nat Commun *11*, 222. 10.1038/s41467-019-13940-6.

12. de Wit, E., Feldmann, F., Cronin, J., Jordan, R., Okumura, A., Thomas, T., Scott, D., Cihlar, T., and Feldmann, H. (2020). Prophylactic and therapeutic remdesivir (GS-5734) treatment in the rhesus macaque model of MERS-CoV infection. Proc Natl Acad Sci U S A *117*, 6771-6776. 10.1073/pnas.1922083117.

13. Beigel, J.H., Tomashek, K.M., Dodd, L.E., Mehta, A.K., Zingman, B.S., Kalil, A.C., Hohmann, E., Chu, H.Y., Luetkemeyer, A., Kline, S., et al. (2020). Remdesivir for the Treatment of Covid-19 - Final Report. N Engl J Med *383*, 1813-1826. 10.1056/NEJMoa2007764.

14. Olender, S.A., Perez, K.K., Go, A.S., Balani, B., Price-Haywood, E.G., Shah, N.S., Wang, S., Walunas, T.L., Swaminathan, S., Slim, J., et al. (2021). Remdesivir for Severe Coronavirus Disease 2019 (COVID-19) Versus a Cohort Receiving Standard of Care. Clin Infect Dis *73*, e4166-e4174. 10.1093/cid/ciaa1041.

15. Bergmann, C., Guay-Woodford, L.M., Harris, P.C., Horie, S., Peters, D.J.M., and Torres, V.E. (2018). Polycystic kidney disease. Nat Rev Dis Primers *4*, 50. 10.1038/s41572-018-0047-y.

16. The polycystic kidney disease 1 gene encodes a 14 kb transcript and lies within a duplicated region on chromosome 16. The European Polycystic Kidney Disease Consortium. (1994). Cell *77*, 881-894. 10.1016/0092-8674(94)90137-6.

17. Mochizuki, T., Wu, G., Hayashi, T., Xenophontos, S.L., Veldhuisen, B., Saris, J.J., Reynolds, D.M., Cai, Y., Gabow, P.A., Pierides, A., et al. (1996). PKD2, a gene for polycystic kidney disease that encodes an integral membrane protein. Science *272*, 1339-1342. 10.1126/science.272.5266.1339.

18. Formica, C., and Peters, D.J.M. (2020). Molecular pathways involved in injury-repair and ADPKD progression. Cell Signal *72*, 109648. 10.1016/j.cellsig.2020.109648.

19. Torres, V.E., Chapman, A.B., Devuyst, O., Gansevoort, R.T., Grantham, J.J., Higashihara, E., Perrone, R.D., Krasa, H.B., Ouyang, J., and Czerwiec, F.S. (2012). Tolvaptan in patients with autosomal dominant polycystic kidney disease. N Engl J Med *367*, 2407-2418. 10.1056/NEJMoa1205511.

20. Torres, V.E., Chapman, A.B., Devuyst, O., Gansevoort, R.T., Perrone, R.D., Koch, G., Ouyang, J., McQuade, R.D., Blais, J.D., Czerwiec, F.S., and Sergeyeva, O. (2017). Tolvaptan in Later-Stage Autosomal Dominant Polycystic Kidney Disease. N Engl J Med *377*, 1930-1942. 10.1056/NEJMoa1710030.

21. Zhou, J.X., and Torres, V.E. (2023). Autosomal Dominant Polycystic Kidney Disease Therapies on the Horizon. Adv Kidney Dis Health *30*, 245-260. 10.1053/j.akdh.2023.01.003.

22. Mullen, J., Cockell, S.J., Woollard, P., and Wipat, A. (2016). An Integrated Data Driven Approach to Drug Repositioning Using Gene-Disease Associations. PLOS ONE *11*, e0155811. 10.1371/journal.pone.0155811.

23. Uffelmann, E., Huang, Q.Q., Munung, N.S., de Vries, J., Okada, Y., Martin, A.R., Martin, H.C., Lappalainen, T., and Posthuma, D. (2021). Genome-wide association studies. Nature Reviews Methods Primers *1*, 59. 10.1038/s43586-021-00056-9.

24. Visscher, P.M., Wray, N.R., Zhang, Q., Sklar, P., McCarthy, M.I., Brown, M.A., and Yang, J. (2017). 10 Years of GWAS Discovery: Biology, Function, and Translation. Am J Hum Genet *101*, 5-22. 10.1016/j.ajhg.2017.06.005.

25. Stark, R., Grzelak, M., and Hadfield, J. (2019). RNA sequencing: the teenage years. Nature Reviews Genetics *20*, 631-656. 10.1038/s41576-019-0150-2.

26. Musa, A., Ghoraie, L.S., Zhang, S.D., Glazko, G., Yli-Harja, O., Dehmer, M., Haibe-Kains, B., and Emmert-Streib, F. (2018). A review of connectivity map and computational approaches in pharmacogenomics. Brief Bioinform *19*, 506-523. 10.1093/bib/bbw112.

27. Lamb, J., Crawford, E.D., Peck, D., Modell, J.W., Blat, I.C., Wrobel, M.J., Lerner, J., Brunet, J.P., Subramanian, A., Ross, K.N., et al. (2006). The Connectivity Map: using gene-expression signatures to connect small molecules, genes, and disease. Science *313*, 1929-1935. 10.1126/science.1132939.

28. Vidović, D., Koleti, A., and Schürer, S.C. (2014). Large-scale integration of small molecule-induced genome-wide transcriptional responses, Kinome-wide binding affinities and cell-growth inhibition profiles reveal global trends characterizing systems-level drug action. Front Genet *5*, 342. 10.3389/fgene.2014.00342.

29. Chen, S., Huang, L., Zhou, S., Zhang, Q., Ruan, M., Fu, L., Yang, B., Xu, D., Mei, C., and Mao, Z. (2021). NS398 as a potential drug for autosomal-dominant polycystic kidney disease: Analysis using bioinformatics, and zebrafish and mouse models. J Cell Mol Med *25*, 9597-9608. 10.1111/jcmm.16903.

30. Wilk, E.J., Howton, T.C., Fisher, J.L., Oza, V.H., Brownlee, R.T., McPherson, K.C., Cleary, H.L., Yoder, B.K., George, J.F., Mrug, M., and Lasseigne, B.N. (2023). Prioritized polycystic kidney disease drug targets and repurposing candidates from pre-cystic and cystic mouse Pkd2 model gene expression reversion. Mol Med *29*, 67. 10.1186/s10020-023-00664-z.

31. Malas, T.B., Leonhard, W.N., Bange, H., Granchi, Z., Hettne, K.M., Van Westen, G.J.P., Price, L.S., t Hoen, P.A.C., and Peters, D.J.M. (2020). Prioritization of novel ADPKD drug candidates from disease-stage specific gene expression profiles. EBioMedicine *51*, 102585. 10.1016/j.ebiom.2019.11.046.

32. Booij, T.H., Bange, H., Leonhard, W.N., Yan, K., Fokkelman, M., Kunnen, S.J., Dauwerse, J.G., Qin, Y., van de Water, B., van Westen, G.J.P., et al. (2017). High-Throughput Phenotypic Screening of Kinase Inhibitors to Identify Drug Targets for Polycystic Kidney Disease. SLAS Discovery *22*, 974-984. https://doi.org/10.1177/2472555217716056.

33. Dagorn, P.G., Buchholz, B., Kraus, A., Batchuluun, B., Bange, H., Blockken, L., Steinberg, G.R., Moller, D.E., and Hallakou-Bozec, S. (2023). A novel direct adenosine monophosphate kinase activator ameliorates disease progression in preclinical models of Autosomal Dominant Polycystic Kidney Disease. Kidney International *103*, 917-929. https://doi.org/10.1016/j.kint.2023.01.026.

34. Lantinga-van Leeuwen, I.S., Leonhard, W.N., van de Wal, A., Breuning, M.H., Verbeek, S., de Heer, E., and Peters, D.J. (2006). Transgenic mice expressing tamoxifen-inducible Cre for somatic gene modification in renal epithelial cells. Genesis *44*, 225-232. 10.1002/dvg.20207.

35. Lantinga-van Leeuwen, I.S., Leonhard, W.N., van der Wal, A., Breuning, M.H., de Heer, E., and Peters, D.J. (2007). Kidney-specific inactivation of the Pkd1 gene induces rapid cyst formation in developing kidneys and a slow onset of disease in adult mice. Hum Mol Genet *16*, 3188-3196. 10.1093/hmg/ddm299.

36. Leonhard, W.N., Kunnen, S.J., Plugge, A.J., Pasternack, A., Jianu, S.B., Veraar, K., El Bouazzaoui, F., Hoogaars, W.M., Ten Dijke, P., Breuning, M.H., et al. (2016). Inhibition of Activin Signaling Slows Progression of Polycystic Kidney Disease. J Am Soc Nephrol *27*, 3589-3599. 10.1681/asn.2015030287.

37. Leonhard, W.N., Song, X., Kanhai, A.A., Iliuta, I.A., Bozovic, A., Steinberg, G.R., Peters, D.J.M., and Pei, Y. (2019). Salsalate, but not metformin or canagliflozin, slows kidney cyst growth in an adult-onset mouse model of polycystic kidney disease. EBioMedicine *47*, 436-445. 10.1016/j.ebiom.2019.08.041.

38. Leonhard, W.N., van der Wal, A., Novalic, Z., Kunnen, S.J., Gansevoort, R.T., Breuning, M.H., de Heer, E., and Peters, D.J. (2011). Curcumin inhibits cystogenesis by simultaneous interference of multiple signaling pathways: in vivo evidence from a Pkd1-deletion model. Am J Physiol Renal Physiol *300*, F1193-1202. 10.1152/ajprenal.00419.2010.

39. Lorrain, D.S., Bain, G., Correa, L.D., Chapman, C., Broadhead, A.R., Santini, A.M., Prodanovich, P.P., Darlington, J.V., Stock, N.S., Zunic, J., et al. (2010). Pharmacology of AM803, a novel selective five-lipoxygenase-activating protein (FLAP) inhibitor in rodent models of acute inflammation. European Journal of Pharmacology *640*, 211-218. https://doi.org/10.1016/j.ejphar.2010.05.003.

40. Gresele, P., Arnout, J., Coene, M.C., Deckmyn, H., and Vermylen, J. (1986). Leukotriene B4 production by stimulated whole blood: Comparative studies with isolated polymorphonuclear cells. Biochemical and Biophysical Research Communications *137*, 334-342. https://doi.org/10.1016/0006-291X(86)91215-5.

41. Spithoven, E.M., Kramer, A., Meijer, E., Orskov, B., Wanner, C., Abad, J.M., Aresté, N., Alonso de la Torre, R., Caskey, F., Couchoud, C., et al. (2014). Renal replacement therapy for autosomal dominant polycystic kidney disease (ADPKD) in Europe: prevalence and survival—an analysis of data from the ERA-EDTA Registry. Nephrology Dialysis Transplantation *29*, iv15-iv25. 10.1093/ndt/gfu017.

42. Abramovitz, M., Wong, E., Cox, M.E., Richardson, C.D., Li, C., and Vickers, P.J. (1993). 5-lipoxygenase-activating protein stimulates the utilization of arachidonic acid by 5-lipoxygenase. Eur J Biochem *215*, 105-111. 10.1111/j.1432-1033.1993.tb18012.x.

43. Peters-Golden, M., and Henderson, W.R. (2007). Leukotrienes. New England Journal of Medicine *357*, 1841-1854. 10.1056/NEJMra071371.

44. Di Gennaro, A., and Haeggström, J.Z. (2012). Chapter Two - The Leukotrienes: Immune-Modulating Lipid Mediators of Disease. In Advances in Immunology, F.W. Alt, ed. (Academic Press), pp. 51-92. https://doi.org/10.1016/B978-0-12-394300-2.00002-8.

45. Novella-Rausell, C., Grudniewska, M., Peters, D.J.M., and Mahfouz, A. (2023). A comprehensive mouse kidney atlas enables rare cell population characterization and robust marker discovery. iScience *26*, 106877. 10.1016/j.isci.2023.106877.

46. Luck, K., Kim, D.K., Lambourne, L., Spirohn, K., Begg, B.E., Bian, W., Brignall, R., Cafarelli, T., Campos-Laborie, F.J., Charloteaux, B., et al. (2020). A reference map of the human binary protein interactome. Nature *580*, 402-408. 10.1038/s41586-020-2188-x.

47. Wang, J., Huo, K., Ma, L., Tang, L., Li, D., Huang, X., Yuan, Y., Li, C., Wang, W., Guan, W., et al. (2011). Toward an understanding of the protein interaction network of the human liver. Mol Syst Biol *7*, 536. 10.1038/msb.2011.67.

48. Jouret, F., and Devuyst, O. (2020). Targeting chloride transport in autosomal dominant polycystic kidney disease. Cellular Signalling *73*, 109703. https://doi.org/10.1016/j.cellsig.2020.109703.

49. Podrini, C., Cassina, L., and Boletta, A. (2020). Metabolic reprogramming and the role of mitochondria in polycystic kidney disease. Cellular Signalling *67*, 109495. https://doi.org/10.1016/j.cellsig.2019.109495.

50. Montford, J.R., Bauer, C., Dobrinskikh, E., Hopp, K., Levi, M., Weiser-Evans, M., Nemenoff, R., and Furgeson, S.B. (2019). Inhibition of 5-lipoxygenase decreases renal fibrosis and progression of chronic kidney disease. Am J Physiol Renal Physiol *316*, F732-f742. 10.1152/ajprenal.00262.2018.

51. Song, C.J., Li, Z., Ahmed, U.K.B., Bland, S.J., Yashchenko, A., Liu, S., Aloria, E.J., Lever, J.M., Gonzalez, N.M., Bickel, M.A., et al. (2022). A Comprehensive Immune Cell Atlas of Cystic Kidney Disease Reveals the Involvement of Adaptive Immune Cells in Injury-Mediated Cyst Progression in Mice. J Am Soc Nephrol *33*, 747-768. 10.1681/asn.2021030278.

52. Zimmerman, K.A., Bentley, M.R., Lever, J.M., Li, Z., Crossman, D.K., Song, C.J., Liu, S., Crowley, M.R., George, J.F., Mrug, M., and Yoder, B.K. (2019). Single-Cell RNA Sequencing Identifies Candidate Renal Resident Macrophage Gene Expression Signatures across Species. Journal of the American Society of Nephrology *30*, 767-781. 10.1681/asn.2018090931.

53. Happé, H., and Peters, D.J. (2014). Translational research in ADPKD: lessons from animal models. Nat Rev Nephrol *10*, 587-601. 10.1038/nrneph.2014.137.

54. Karihaloo, A. (2015). Role of Inflammation in Polycystic Kidney Disease. In Polycystic Kidney Disease, X. Li, ed. (Codon Publications Copyright: The Authors.). 10.15586/codon.pkd.2015.ch14.

55. Bain, G., King, C.D., Schaab, K., Rewolinski, M., Norris, V., Ambery, C., Bentley, J., Yamada, M., Santini, A.M., van de Wetering de Rooij, J., et al. (2013). Pharmacodynamics, pharmacokinetics and safety of GSK2190915, a novel oral anti-inflammatory 5-lipoxygenase-activating protein inhibitor. Br J Clin Pharmacol *75*, 779-790. 10.1111/j.1365-2125.2012.04386.x.

56. Kent, S.E., Boyce, M., Diamant, Z., Singh, D., O'Connor, B.J., Saggu, P.S., and Norris, V. (2013). The 5-lipoxygenase-activating protein inhibitor, GSK2190915, attenuates the early and late responses to inhaled allergen in mild asthma. Clin Exp Allergy *43*, 177-186. 10.1111/cea.12002.

57. Follows, R.M., Snowise, N.G., Ho, S.Y., Ambery, C.L., Smart, K., and McQuade, B.A. (2013). Efficacy, safety and tolerability of GSK2190915, a 5-lipoxygenase activating protein inhibitor, in adults and adolescents with persistent asthma: a randomised dose-ranging study. Respir Res *14*, 54. 10.1186/1465-9921-14-54.

58. Chaudhuri, R., Norris, V., Kelly, K., Zhu, C.Q., Ambery, C., Lafferty, J., Cameron, E., and Thomson, N.C. (2014). Effects of a FLAP inhibitor, GSK2190915, in asthmatics with high sputum neutrophils. Pulm Pharmacol Ther *27*, 62-69. 10.1016/j.pupt.2013.11.007.

59. Singh, D., Boyce, M., Norris, V., Kent, S.E., and Bentley, J.H. (2013). Inhibition of the early asthmatic response to inhaled allergen by the 5-lipoxygenase activating protein inhibitor GSK2190915: a dose-response study. Int J Gen Med *6*, 897-903. 10.2147/ijgm.S51364.

60. Kent, S.E., Bentley, J.H., Miller, D., Sterling, R., Menendez, R., Tarpay, M., Pearlman, D.S., and Norris, V. (2014). The effect of GSK2190915, a 5-lipoxygenase-activating protein inhibitor, on exercise-induced bronchoconstriction. Allergy Asthma Proc *35*, 126-133. 10.2500/aap.2014.35.3723.

61. Reagan-Shaw, S., Nihal, M., and Ahmad, N. (2008). Dose translation from animal to human studies revisited. Faseb j *22*, 659-661. 10.1096/fj.07-9574LSF.